Supplementary Information for

Substantial thermal conductivity reduction in mischmetal skutterudites Mm_xCoSb_3 prepared under high-pressure conditions, due to uneven distribution of the rare-earth elements

J. Gainza,[a,c] F. Serrano-Sánchez,[a] J. Prado-Gonjal, [a,b] N. M. Nemes,[c] N. Biskup,[c,d] O. J. Dura,[e] J.L. Martínez,[a] F. Fauth,[f] J.A. Alonso[a]*

[a] *Instituto de Ciencias de Materiales de Madrid (ICMM). Consejo Superior de Investigaciones Científicas (CSIC). Sor Juana Inés de la Cruz 3, E-28049, Madrid, Spain.*

[b] *Departamento de Química Inorgánica, Universidad Complutense de Madrid, E-28040 Madrid, Spain*

[c] *Departamento de Física de Materiales, Universidad Complutense de Madrid, E-28040 Madrid, Spain*

[d] *Instituto Pluridisciplinar, Universidad Complutense de Madrid, E-28040, Spain.*

[e] *Departamento de Física Aplicada, Universidad de Castilla-La Mancha, Ciudad Real, E-13071, Spain*

[f] *Institut Laue Langevin, BP 156X, Grenoble, F-38042, France*

[g] *CELLS–ALBA synchrotron, Cerdanyola del Valles, Barcelona, E-08290, Spain*

Figure S1. Laboratory X-ray powder diffraction patterns for different $Mm_xCo_4Sb_{12}$ compositions (x = 0.15, 0.2, 0.5). Observed (red crosses), calculated (black solid line), and difference (blue line at the bottom). Allowed Bragg reflections are indicated by the green tick marks.

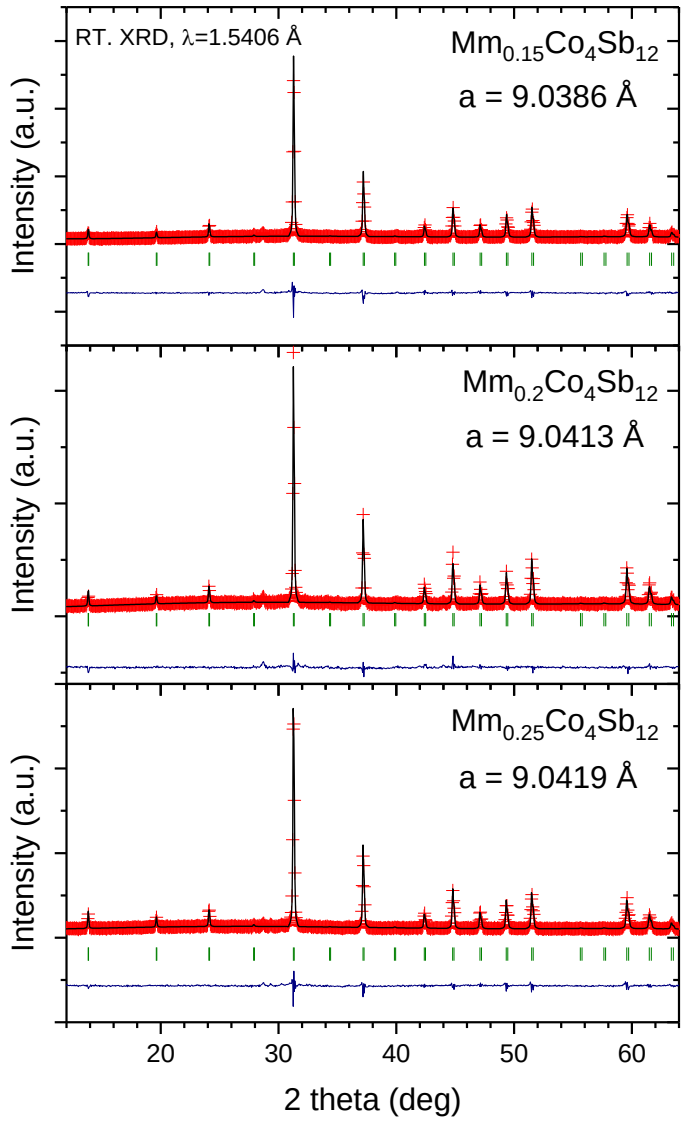

Synchrotron Rietveld refinements

Table S1. Crystallographic parameters of $Mm_{0.5}Co_4Sb_{12}$ from SXRD data at different temperatures. SG: $Im\bar{3}$.

Temperature (K)	**RT**		**473**		**673**		**873**		**1073**	
Lattice parameter, *a* / Å	9.04724(4)	9.03936(4)	9.06616(3)	9.05797(3)	9.08362(3)	9.07516(3)	9.10133(3)	9.09304(2)	9.11954(5)	9.11222(4)
y (Sb)	0.33559(15)	0.33478(15)	0.33535(13)	0.33494(12)	0.33517(15)	0.33462(15)	0.33519(17)	0.33456(11)	0.3349(3)	0.33431(19)
z (Sb)	0.15833(14)	0.15759(14)	0.15817(12)	0.15775(12)	0.15830(15)	0.15768(14)	0.15834(16)	0.15777(10)	0.1585(3)	0.15790(19)
Occ. Sb (<1)	0.967(8)	0.978(7)	0.967	0.978	0.967	0.978	0.967	0.978	0.967	0.978
Occ. Ce (<1)		0.050(9)		0.050		0.050		0.050		0.050
Occ. R (<1)	0.084(9)		0.084		0.084		0.084		0.084	
U_{11} (Co) / Å^2 *	0.0050(4)		0.0075(3)		0.0108(4)		0.0147(4)		0.0190(7)	
U_{12} (Co) / Å^2 **	0.0000(5)		0.0002(5)		0.0000(7)		0.0004(6)		-0.0002(12)	
U_{11} (Sb) / Å^2 ***	0.0055(4)		0.0073(3)		0.0106(5)		0.0145(4)		0.0177(8)	
U_{22} (Sb) / Å^2	0.0087(5)		0.0132(4)		0.0187(6)		0.0245(6)		0.0312(11)	
U_{33} (Sb) / Å^2	0.0064(4)		0.0095(4)		0.0145(6)		0.0190(5)		0.0238(10)	
U_{23} (Sb) / Å^2	0.0011(3)		0.0018(3)		0.0020(4)		0.0029(4)		0.0035(7)	
U_{11} (R) / Å^2 ****	0.037(13)		0.042(9)		0.044(12)		0.11(2)		0.11(4)	
R_p (%)	6.16		5.41		5.92		5.99		6.34	
R_{wp} (%)	7.80		6.91		8.30		8.01		9.40	
R_{exp} (%)	5.62		4.45		4.39		4.36		4.44	
χ^2 (%)	1.93		2.41		3.58		3.37		4.47	
R_I	2.12	1.63	2.15	1.92	2.45	2.11	3.33	1.62	4.42	2.42
Sb at 24*g*, (*0*,*y*,*z*); Co at 8*c* (*¼*,*¼*,*¼*); Mm = La, Ce at 2a (0,0,0) *Anisotropic U Co:* * $U_{11} = U_{22} = U_{33}$;** $U_{12} = U_{23} = U_{13}$; Sb:*** $U_{12} = U_{13} = 0$; La:****$U_{11} = U_{22} = U_{33}$										

Figure S2. $Mm_{0.5}Co_4Sb_{12}$ Synchrotron X-ray Powder Diffraction patterns at different temperatures. Observed (red crosses), calculated (black solid line), and difference (blue line at the bottom). Allowed Bragg reflections are indicated by the green tick marks.

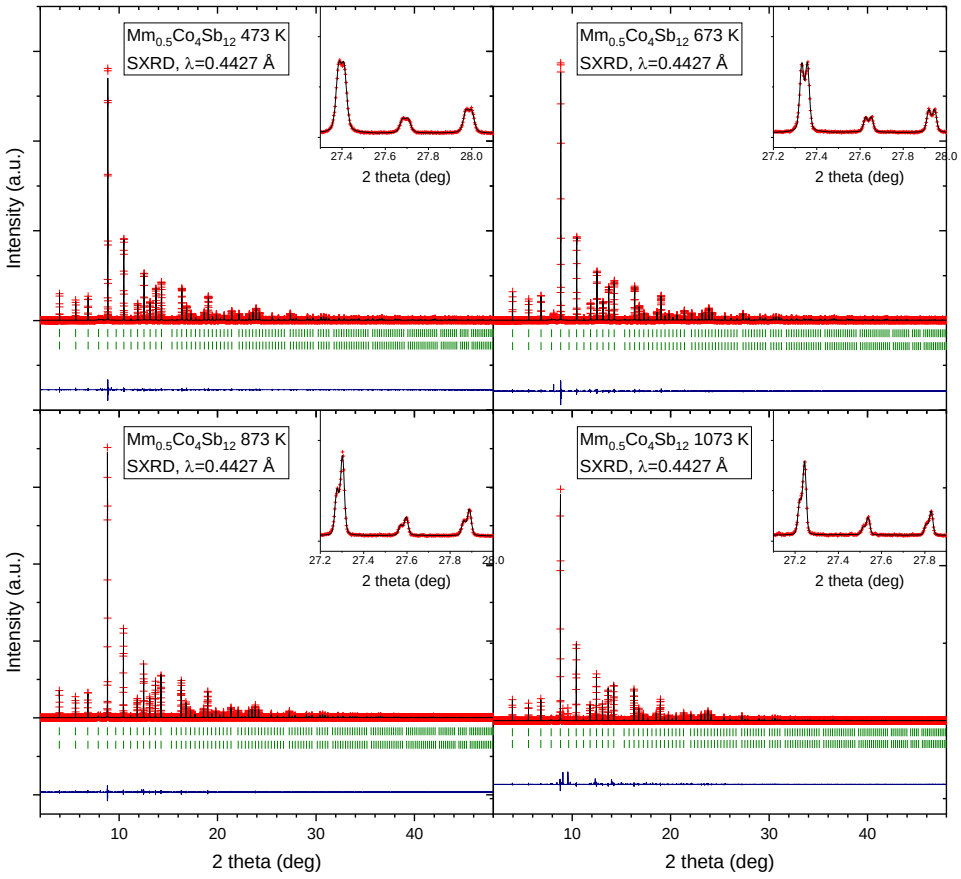

Table S2. Crystallographic parameters of $Mm_{0.5}Co_4Sb_{12}$ from SXRD data at different temperatures including refined occupancy factors at high temperature. SG: $Im\bar{3}$.

Temperature (K)	**RT**		**473**		**673**		**873**		**1073**	
Lattice parameter, *a* / Å	9.04724(4)	9.03936(4)	9.06614(3)	9.05795(3)	9.08361(3)	9.07516(3)	9.10131(3)	9.09303(2)	9.11954(5)	9.11222(4)
y (Sb)	0.33559(15)	0.33478(15)	0.33530(13)	0.33480(13)	0.33511(15)	0.33457(15)	0.33501(17)	0.33443(11)	0.3346(3)	0.33410(19)
z (Sb)	0.15833(14)	0.15759(14)	0.15815(12)	0.15767(12)	0.15829(15)	0.15769(14)	0.15834(16)	0.15779(10)	0.1586(3)	0.15794(18)
Occ. Sb (<1)	0.967(8)	0.978(7)	0.970(6)	0.985(6)	0.975(7)	0.988(7)	1.002(8)	0.996(6)	1.015(16)	1.016(10)
Occ. Ce (<1)		0.050(9)		0.035(7)		0.035(7)		0.019(5)		0.021(8)
Occ. R (<1)	0.084(9)		0.082(7)		0.079(9)		0.073(9)		0.056(16)	
Phase Abundance /%	50.1(9)	49.9(9)	50.6(8)	49.4(8)	49.9(9)	50.1(9)	34.8(6)	65.2(9)	30(1)	70(2)
U_{11} (Co) / Å^2 *	0.0050(4)		0.0071(4)		0.0101(5)		0.0129(5)		0.0157(9)	
U_{12} (Co) / Å^2 **	0.0000(5)		0.0002(5)		0.0001(7)		0.0004(6)		-0.0001(12)	
U_{11} (Sb) / Å^2 ***	0.0055(4)		0.0073(3)		0.0107(5)		0.0147(4)		0.0180(8)	
U_{22} (Sb) / Å^2	0.0087(5)		0.0132(4)		0.0188(6)		0.0248(6)		0.0317(11)	
U_{33} (Sb) / Å^2	0.0064(4)		0.0094(4)		0.0144(6)		0.0189(5)		0.0238(10)	
U_{23} (Sb) / Å^2	0.0011(3)		0.0018(3)		0.0021(4)		0.0030(4)		0.0037(7)	
U_{11} (R) / Å^2 ****	0.037(13)		0.024(10)		0.026(13)		0.023(15)		0.00(2)	
R_p (%)	6.16		5.38		5.91		5.99		6.39	
R_{wp} (%)	7.80		6.90		8.30		7.95		9.30	
R_{exp} (%)	5.62		4.45		4.39		4.36		4.44	
χ^2 (%)	1.93		2.40		3.58		3.32		4.38	
R_I	2.12	1.63	2.11	1.90	2.42	2.07	3.23	1.69	4.33	2.50
Sb at 24*g*, (*0*,*y*,*z*); Co at 8*c* (*¼*,*¼*,*¼*); Mm = La, Ce at 2a (0,0,0) *Anisotropic U Co:* * $U_{11} = U_{22} = U_{33}$;** $U_{12} = U_{23} = U_{13}$; Sb:*** $U_{12} = U_{13} = 0$; La:****$U_{11} = U_{22} = U_{33}$										

Figure S3. Temperature evolution of the split diffraction peaks in SXRD patterns for $Mm_{0.5}Co_4Sb_{12}$.

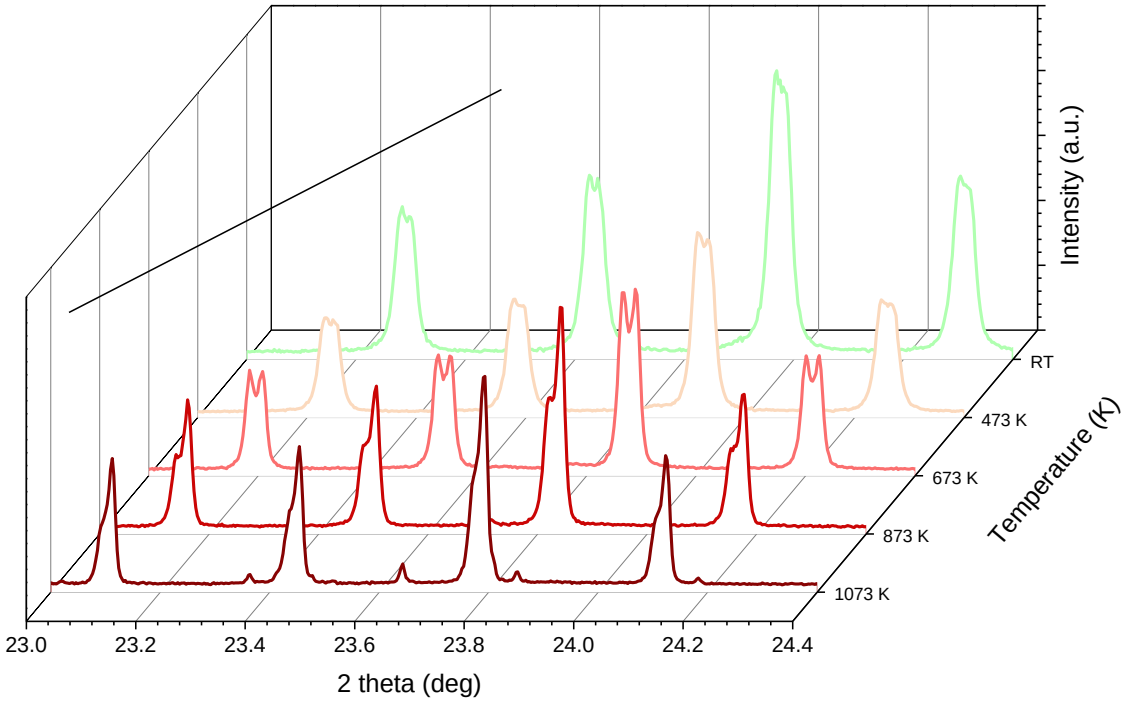

Figure S4. SEM images of as-grown pellets of $Mm_{0.2}Co_4Sb_{12}$. a) x8000, b) x9000 c) x7000, d) x6000, f) x1500 and g) x5000 magnification.

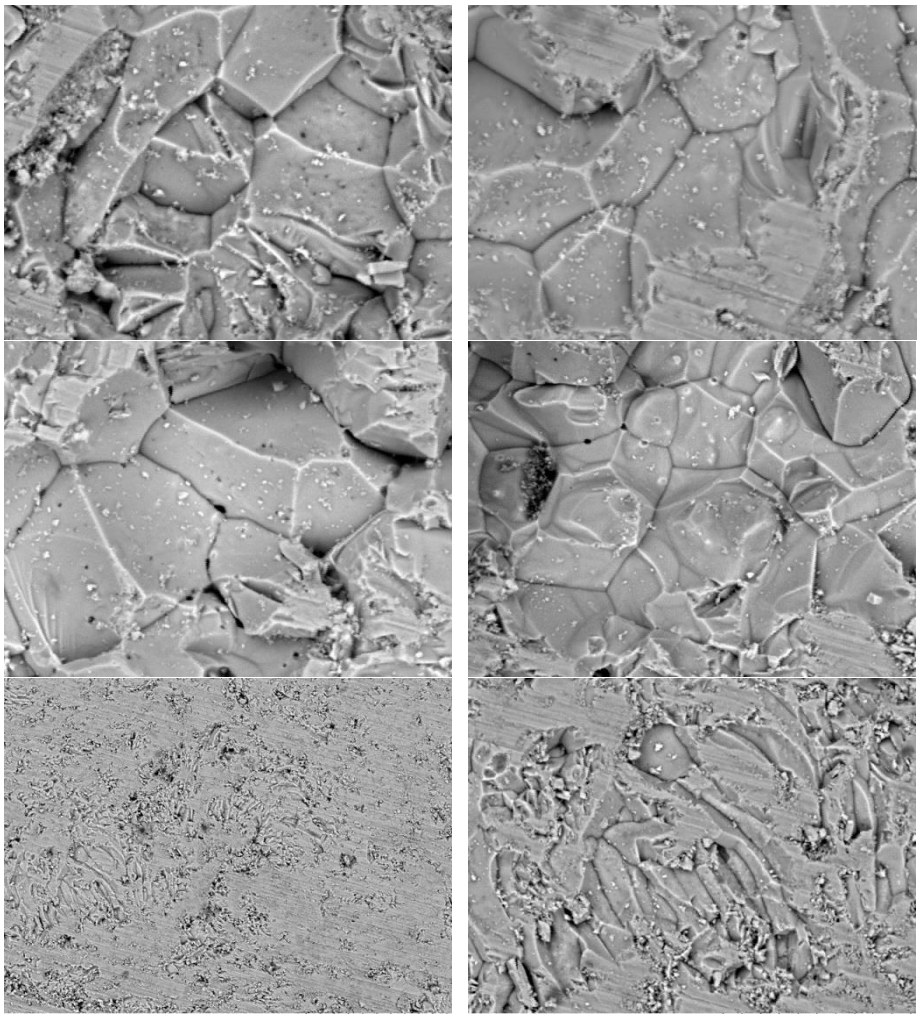

Figure S5. Elemental mapping of another grain based on EELS analysis, including: ADF image taken during the EELS acquisition. Red and green rectangles depict the regions from which the two spectra are taken. Two spectra with elemental edges indicated. Elemental maps of antimony (yellow), cobalt (blue), lanthanum (green) and cerium (red).

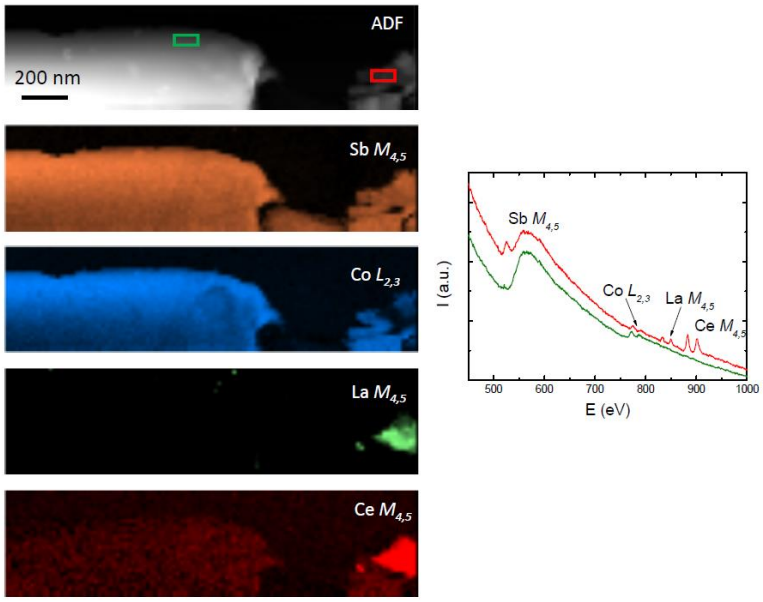

Figure S6. $Mm_{0.5}Co_4Sb_{12}$ before and after the annealing thermal treatment. We can see how thermal conductivity rises due to a more homogeneous distribution of the mischmetal content.

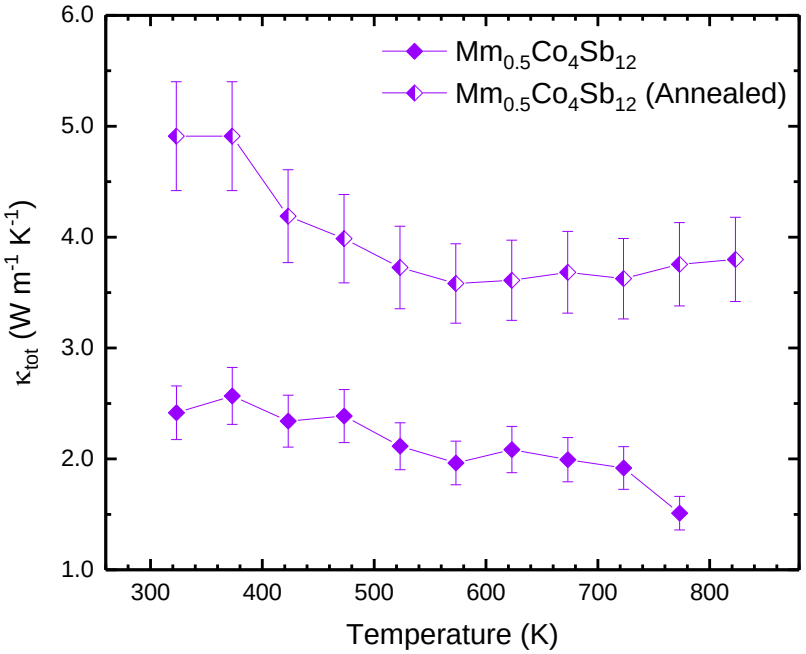

Figure S7. ZT of $Mm_{0.5}Co_4Sb_{12}$ before and after the annealing thermal treatment compared to unfilled $CoSb_3$ prepared under high pressure and by conventional methods. ZT calculation have been performed using the same power factor for the annealed and unannealed $Mm_{0.5}Co_4Sb_{12}$ samples.